JHWCR JOURNAL OF HEALTH, WELLNESS AND COMMUNITY RESEARCH 3007-0570

https://doi.org/10.61919/za034z14

Original Article

Comparative Antimicrobial Efficacy of Chitosan–Graphene Oxide and Chitosan–Reduced Graphene Oxide Membranes

Muhammad Umar[1], Amjad Ali[2], Aijaz Ahmed Bhutto[3], Sikander Zafar Siddiqui[4], Z.H Shar[3], Anosha Aamir[5], Mumtaz Hussain[6]

[1] Department of Biochemistry, University of Narowal, Narowal, Pakistan, https://orcid.org/0009-0006-4822-366X
[2] MPhil, Centre for Biotechnology and Microbiology, University of Swat, Pakistan, https://orcid.org/0009-0007-2140-5102
[3] Dr. M.A Kazi Institute of Chemistry, University of Sindh, Jamshoro, Pakistan
[4] MS in Biotechnology for Food Sciences, University of Padova, Italy; Product Development Manager, SG Allied Businesses Limited
[5] MPhil Research Fellow in Molecular Medicine, PCMD, ICCBS, University of Karachi, Karachi, Pakistan
[6] Department of Chemistry, University of Karachi, Karachi, Pakistan

***Corresponding author: Muhammad Umar, m.umarshafiq431@gmail.com**

"Cite this Article" Received: 07 January 2026; **Accepted**: 14 April 2026; **Published**: 04 May 2026

Author Contributions: Concept: MU; Design: AA and AAB; Data Collection: SZS and ZAHS; Analysis: AA and AM; Drafting: MU and MH. **Ethical Approval**: University of Narowal, Narowal, Pakistan **Informed Consent**: Written informed consent was obtained from all participants; **Conflict of Interest**: The authors declare no conflict of interest. **Funding**: No external funding; **Data Availability**: Available from the corresponding author on reasonable request; **Acknowledgments**: N/A.

ABSTRACT

Background: Hospital-associated infections and antimicrobial resistance remain major clinical challenges, particularly in settings with high bacterial burden and frequent antibiotic exposure. Chitosan is a biocompatible antimicrobial polymer, but its limited mechanical stability restricts broader biomedical use. Graphene oxide and reduced graphene oxide may improve chitosan membrane performance, although their different oxidation states may produce distinct antimicrobial, mechanical, and biological effects. Objective: To compare the antimicrobial efficacy, mechanical stability, and basic biocompatibility of pure chitosan, chitosan–graphene oxide, and chitosan–reduced graphene oxide membranes. Methods: This comparative experimental study evaluated three membrane groups prepared by solution casting. Physical and mechanical properties were assessed using thickness, water uptake, tensile strength, elongation at break, and surface pH. Antimicrobial activity was tested against Staphylococcus aureus, Escherichia coli, Pseudomonas aeruginosa, and Klebsiella pneumoniae using agar diffusion and direct-contact viable count methods. Cell viability and hemolysis were used for basic compatibility assessment. Results: Chitosan–GO showed the highest tensile strength (32.7 ± 2.1 MPa), largest inhibition zones, and greatest 24-hour bacterial reduction (94.3 ± 2.8%), followed by chitosan–rGO and pure chitosan. Pure chitosan had the highest cell viability (93.4 ± 2.5%), while chitosan–GO retained acceptable viability (88.7 ± 2.8%) and lower hemolysis than chitosan–rGO. Conclusion: Chitosan–graphene oxide demonstrated the best overall balance of antimicrobial efficacy, mechanical strength, and biological compatibility, supporting its potential for antimicrobial biomaterial development. Keywords: Chitosan membrane; graphene oxide; reduced graphene oxide; antimicrobial efficacy; hospital pathogens; biomaterials; mechanical stability; biocompatibility.

INTRODUCTION

Antimicrobial resistance has become one of the most serious threats to modern health care, particularly in hospital settings where vulnerable patients are exposed to invasive procedures, open wounds, surgical sites, indwelling devices, and prolonged antibiotic therapy. The global burden of bacterial antimicrobial resistance in 2019 demonstrated that resistant infections are no longer limited to microbiological concern but represent a major contributor to morbidity and mortality across health systems (1). This challenge is especially relevant in Pakistan, where tertiary-care hospitals face high infectious disease pressure, frequent empirical antibiotic use, delayed culture-guided treatment, and documented gaps in

antimicrobial stewardship practice (23–25). In such environments, infection-preventive biomaterials that can reduce microbial colonization before progression to established infection may offer an important supportive strategy alongside conventional antimicrobial control.

Chitosan has gained considerable attention as a biomedical polymer because of its biodegradability, biocompatibility, film-forming capacity, and intrinsic antimicrobial activity. Its cationic structure enables interaction with negatively charged bacterial cell surfaces, leading to altered membrane permeability, disruption of nutrient transport, and inhibition of microbial viability (17–21). These properties make chitosan suitable for wound-contact membranes, antimicrobial films, and temporary biomedical interfaces. However, pure chitosan membranes often show limited tensile strength, variable moisture stability, and reduced durability under demanding biological conditions, which restricts their independent use in applications requiring both antimicrobial action and mechanical integrity (17–21).

Graphene-based nanomaterials have been explored as reinforcing agents to overcome these limitations. Graphene oxide contains oxygenated functional groups, including hydroxyl, epoxy, and carboxyl groups, which improve hydrophilicity, dispersion, and interfacial interaction with polymer matrices such as chitosan. Reduced graphene oxide, produced by partial removal of these oxygen-containing groups, has different surface chemistry, lower hydrophilicity, altered sheet aggregation behavior, and distinct biological interactions (2,3,11,22). Although both materials belong to the graphene family, their oxidation states may substantially influence membrane morphology, bacterial contact, mechanical reinforcement, water uptake, and host-cell compatibility.

Previous studies have shown that graphene oxide and graphene-based composites can inhibit bacterial growth through membrane stress, physical wrapping or trapping, oxidative injury, and disruption of cellular integrity (2–6). Chitosan–graphene oxide films have also demonstrated improved structural properties and biological performance in biomedical applications (7–16). However, findings across graphene systems are not uniform because antimicrobial effects depend on oxidation state, surface chemistry, concentration, dispersion quality, sheet size, exposure time, and bacterial strain. Despite growing evidence on graphene-reinforced chitosan biomaterials, direct comparative evidence between chitosan–graphene oxide and chitosan–reduced graphene oxide membranes under the same experimental framework remains limited. This knowledge gap is important because treating graphene oxide and reduced graphene oxide as interchangeable materials may lead to inaccurate assumptions about antimicrobial efficacy, mechanical stability, and biological safety.

A clinically useful antimicrobial membrane must provide more than bacterial inhibition alone. It should combine effective contact-based antimicrobial action with acceptable tensile strength, controlled water uptake, structural uniformity, and biocompatibility. This balance is particularly important for hospital-relevant applications such as wound-care materials and temporary antimicrobial surfaces, where excessive cytotoxicity or poor mechanical behavior would limit practical translation. Because tertiary-care hospitals in Sindh, Pakistan, continue to face substantial infectious disease burden and antimicrobial resistance concerns, locally relevant evaluation of low-cost antimicrobial biomaterials is scientifically and clinically justified (23–25).

Therefore, the present comparative experimental study was designed to evaluate the antimicrobial, mechanical, and basic biocompatibility performance of pure chitosan, chitosan–graphene oxide, and chitosan–reduced graphene oxide membranes. The study specifically examined whether the oxidation state of graphene influences membrane behavior against common hospital bacterial isolates, including Staphylococcus aureus, Escherichia coli, Pseudomonas aeruginosa, and Klebsiella pneumoniae. The primary hypothesis was that chitosan–graphene oxide membranes would demonstrate superior antimicrobial efficacy and mechanical stability compared with chitosan–reduced graphene oxide and pure chitosan membranes, while maintaining an acceptable biocompatibility profile.

MATERIALS AND METHODS

This comparative experimental study evaluated three membrane systems: pure chitosan membrane, chitosan–graphene oxide membrane, and chitosan–reduced graphene oxide membrane. The study was designed to determine whether the oxidation state of graphene reinforcement influenced antimicrobial activity, physical stability, mechanical behavior, and basic biocompatibility. Membrane preparation, characterization, antimicrobial testing, and biological compatibility assessment were conducted under standardized laboratory conditions, while clinically relevant bacterial isolates were obtained with support from selected tertiary-care hospitals in Sindh, Pakistan. The total study duration was six months, during which material procurement, membrane fabrication, bacterial confirmation, antimicrobial testing, mechanical evaluation, and biocompatibility assessment were completed.

Medium-molecular-weight chitosan with a high degree of deacetylation was used as the base polymer. Glacial acetic acid was used for chitosan dissolution, while analytical-grade graphene oxide and reduced graphene oxide powders were used as reinforcing nanomaterials. Sodium hydroxide and distilled water were used for membrane neutralization and washing, and glycerol was added as a plasticizing agent to improve film flexibility and reduce brittleness. Microbiological testing was performed using Mueller–Hinton agar, nutrient agar, nutrient broth, phosphate-buffered saline, sterile swabs, micropipettes, Petri plates, and standard microbiological reagents.

Clinical bacterial isolates were selected according to their relevance to hospital-associated infections. The tested organisms included Staphylococcus aureus, Escherichia coli, Pseudomonas aeruginosa, and Klebsiella pneumoniae. Only pure, actively growing cultures were included. Isolates were subcultured and confirmed using standard microbiological procedures, including Gram staining and routine biochemical identification where required. Before antimicrobial testing, bacterial suspensions were standardized to approximately 0.5 McFarland turbidity to ensure comparable inoculum density across all experimental groups.

The pure chitosan membrane was prepared by dissolving chitosan powder in 1% acetic acid under continuous magnetic stirring until a homogeneous viscous solution was obtained. A fixed amount of glycerol was added to improve membrane flexibility. The solution was filtered to remove undissolved particles and air bubbles, poured onto clean leveled casting plates, and dried under controlled conditions. After drying, the membrane was carefully peeled, neutralized using dilute sodium hydroxide, repeatedly washed with distilled water until neutral pH was achieved, dried again, and stored in sterile polythene sheets until testing.

The chitosan–graphene oxide membrane was prepared by dispersing a fixed amount of graphene oxide in distilled water through magnetic stirring followed by sonication to reduce aggregation and improve uniformity. The graphene oxide dispersion was gradually added to the chitosan solution under continuous stirring and mixed until a uniform composite solution was obtained. The mixture was cast, dried, neutralized, washed, and stored using the same procedure as the pure chitosan membrane to minimize procedural variation between groups.

The chitosan–reduced graphene oxide membrane was prepared using the same casting approach. Reduced graphene oxide was dispersed in distilled water using extended stirring and sonication because of its relatively lower hydrophilicity and greater tendency toward aggregation. The dispersion was slowly incorporated into the chitosan solution under continuous stirring, followed by casting, drying, neutralization, washing, and storage under identical conditions. All membranes were prepared with comparable target thickness, and circular discs of equal diameter were cut under sterile conditions for antimicrobial testing.

The experimental groups were defined as Group A, pure chitosan membrane; Group B, chitosan–graphene oxide membrane; and Group C, chitosan–reduced graphene oxide membrane. Each

membrane group was prepared and tested in repeated experimental replicates to improve reproducibility. Membrane thickness was measured at multiple points using a digital micrometer, and mean thickness was recorded. Water uptake was assessed by weighing dried membrane samples, immersing them in distilled water for a fixed duration, removing surface moisture, and reweighing them to calculate percentage weight gain. Surface pH was measured to confirm that residual acidity or alkalinity did not confound biological response. Mechanical stability was assessed through tensile testing, and tensile strength and elongation at break were recorded as indicators of reinforcement performance.

Antimicrobial activity was assessed using agar diffusion and direct-contact viable count methods. For agar diffusion testing, standardized bacterial inoculum was spread uniformly over Mueller–Hinton agar plates. Sterile membrane discs from each group were placed on the inoculated agar surface and incubated at 37°C for 18–24 hours. After incubation, zones of inhibition were measured in millimeters using a standardized measuring scale. Because membrane-based materials may not diffuse uniformly through agar, direct-contact testing was also performed to provide a more reliable estimate of contact-mediated bacterial reduction.

For viable count testing, membrane samples were placed in direct contact with standardized bacterial suspensions for predetermined exposure periods of 2, 6, and 24 hours. After exposure, surviving bacteria were serially diluted and plated on nutrient agar. Colony-forming units were counted after incubation, and percentage bacterial reduction was calculated by comparing viable counts across membrane groups. The primary antimicrobial outcome was percentage bacterial reduction after 24-hour direct contact. Secondary antimicrobial outcomes included zones of inhibition and surviving bacterial counts for each tested organism.

Biocompatibility was assessed using cell viability and hemocompatibility-related screening. For cell viability assessment, membrane extracts were exposed to cultured cells under controlled conditions, and relative cell viability was recorded as a percentage compared with control conditions. Hemocompatibility was assessed by exposing membrane samples to diluted human blood and calculating hemolysis percentage. These outcomes were included to determine whether improved antimicrobial activity was accompanied by acceptable biological safety.

All experimental data were recorded on structured data sheets and checked for completeness before analysis. Continuous variables, including membrane thickness, water uptake, tensile strength, elongation at break, zones of inhibition, percentage bacterial reduction, surviving bacterial count, cell viability, and hemolysis percentage, were summarized using means and standard deviations. Intergroup comparisons among the three membrane groups were performed using one-way analysis of variance. Where statistically significant differences were observed, post hoc pairwise comparisons were applied to identify differences between pure chitosan, chitosan–graphene oxide, and chitosan–reduced graphene oxide membranes. A p-value of less than 0.05 was considered statistically significant. Analytical interpretation focused on both statistical significance and biological relevance, particularly the balance between antimicrobial efficacy, mechanical performance, and compatibility outcomes.

Permission was obtained from the relevant institutional and hospital authorities before collection and use of clinical bacterial isolates. Standard biosafety procedures were followed during culture handling, membrane exposure testing, incubation, and disposal of infectious material. For blood-contact testing, ethical approval and informed consent procedures were followed according to institutional requirements. Reproducibility was strengthened by using standardized membrane preparation procedures, equal-sized test discs, comparable membrane thickness targets, standardized bacterial inoculum density, repeated experimental measurements, calibrated measurement tools, and structured data recording.

RESULTS

The study compared pure chitosan, chitosan–graphene oxide, and chitosan–reduced graphene oxide membranes for physical stability, antimicrobial performance, and basic biocompatibility. All membranes were successfully fabricated, but graphene-reinforced membranes showed better handling strength than pure chitosan. The chitosan–GO membrane showed the strongest overall profile, while chitosan–rGO improved performance compared with pure chitosan but remained slightly inferior to chitosan–GO in most outcomes. Exact p-values and confidence intervals could not be added because raw replicate-level data were not provided; therefore, the manuscript's reported significance threshold is retained as $p < 0.05$.

Table 1. Physical and Mechanical Characteristics of the Prepared Membranes

Parameter	Chitosan Membrane	Chitosan–GO Membrane	Chitosan–rGO Membrane	Statistical Interpretation
Thickness (mm)	0.23 ± 0.02	0.25 ± 0.01	0.24 ± 0.02	Comparable across groups
Water uptake (%)	148.6 ± 6.4	132.8 ± 5.9	118.4 ± 6.1	$p < 0.05$
Tensile strength (MPa)	21.4 ± 1.8	32.7 ± 2.1	29.3 ± 1.9	$p < 0.05$
Elongation at break (%)	18.2 ± 1.5	24.6 ± 1.7	20.3 ± 1.4	$p < 0.05$
Surface pH	6.4 ± 0.1	6.6 ± 0.1	6.5 ± 0.1	Comparable across groups

Pure chitosan showed the highest water uptake at 148.6 ± 6.4%, indicating greater hydrophilicity but lower dimensional stability. Water uptake decreased to 132.8 ± 5.9% in the chitosan–GO group and 118.4 ± 6.1% in the chitosan–rGO group. Tensile strength increased from 21.4 ± 1.8 MPa in pure chitosan to 32.7 ± 2.1 MPa with GO reinforcement and 29.3 ± 1.9 MPa with rGO reinforcement, showing that both graphene derivatives strengthened the membrane, with GO producing the highest mechanical gain.

Table 2. Zone of Inhibition Produced by Membrane Discs Against Test Bacteria

Test Organism	Chitosan Membrane (mm)	Chitosan–GO Membrane (mm)	Chitosan–rGO Membrane (mm)	Statistical Interpretation
Staphylococcus aureus	9.2 ± 0.8	17.8 ± 1.1	15.6 ± 1.0	$p < 0.05$
Escherichia coli	8.4 ± 0.7	16.9 ± 0.9	14.8 ± 0.8	$p < 0.05$
Pseudomonas aeruginosa	7.1 ± 0.6	14.6 ± 0.8	12.9 ± 0.7	$p < 0.05$
Klebsiella pneumoniae	7.8 ± 0.5	15.4 ± 0.9	13.7 ± 0.8	$p < 0.05$

The inhibition-zone pattern consistently favored chitosan–GO, followed by chitosan–rGO and pure chitosan. Against S. aureus, chitosan–GO produced the largest zone of inhibition at 17.8 ± 1.1 mm, compared with 15.6 ± 1.0 mm for chitosan–rGO and 9.2 ± 0.8 mm for pure chitosan. P. aeruginosa was the least sensitive organism, but chitosan–GO still achieved a zone of 14.6 ± 0.8 mm, more than double the 7.1 ± 0.6 mm observed with pure chitosan.

Table 3. Percentage Bacterial Reduction After Direct Membrane Contact

Time Interval	Chitosan Membrane (%)	Chitosan–GO Membrane (%)	Chitosan–rGO Membrane (%)	Statistical Interpretation
2 hours	28.4 ± 3.1	61.7 ± 4.2	54.8 ± 3.9	$p < 0.05$
6 hours	43.9 ± 3.8	79.6 ± 4.5	71.1 ± 4.1	$p < 0.05$
24 hours	58.7 ± 4.0	94.3 ± 2.8	88.5 ± 3.1	$p < 0.05$

Direct-contact testing showed a time-dependent increase in bacterial reduction across all groups. At 24 hours, chitosan–GO achieved the highest bacterial reduction at 94.3 ± 2.8%, compared with 88.5 ± 3.1% for chitosan–rGO and 58.7 ± 4.0% for pure chitosan. The absolute improvement of chitosan–GO over pure chitosan was 35.6 percentage points, while its improvement over chitosan–rGO was 5.8 percentage points.

Table 4. Mean Surviving Bacterial Count After 24-Hour Contact

Test Organism	Chitosan Membrane (CFU/mL)	Chitosan–GO Membrane (CFU/mL)	Chitosan–rGO Membrane (CFU/mL)	Statistical Interpretation
Staphylococcus aureus	4.8×10^3	3.2×10^2	6.1×10^2	$p < 0.05$
Escherichia coli	5.4×10^3	4.6×10^2	8.3×10^2	$p < 0.05$
Pseudomonas aeruginosa	7.1×10^3	9.8×10^2	1.6×10^3	$p < 0.05$
Klebsiella pneumoniae	6.3×10^3	7.4×10^2	1.2×10^3	$p < 0.05$

After 24 hours, chitosan–GO produced the lowest surviving bacterial counts for all organisms. The lowest count was observed for S. aureus at 3.2×10^2 CFU/mL, while the highest residual count in the GO

group was seen for P. aeruginosa at 9.8 × 10^2 CFU/mL. This confirms that P. aeruginosa remained comparatively resistant, although both graphene-reinforced membranes still substantially reduced bacterial survival compared with pure chitosan.

Table 5. Basic Biocompatibility Assessment of Membrane Groups

Parameter	Chitosan Membrane	Chitosan–GO Membrane	Chitosan–rGO Membrane	Statistical Interpretation
Cell viability (%)	93.4 ± 2.5	88.7 ± 2.8	84.9 ± 3.0	$p < 0.05$
Hemolysis (%)	1.8 ± 0.3	2.6 ± 0.4	3.4 ± 0.5	$p < 0.05$

Pure chitosan showed the highest cell viability at 93.4 ± 2.5% and the lowest hemolysis at 1.8 ± 0.3%, confirming its favorable baseline compatibility. Chitosan–GO retained acceptable cell viability at 88.7 ± 2.8% with hemolysis of 2.6 ± 0.4%, whereas chitosan–rGO showed lower viability at 84.9 ± 3.0% and higher hemolysis at 3.4 ± 0.5%. These findings suggest that GO provided a better balance between antimicrobial enhancement and biological safety than rGO.

Table 6. Summary of Intergroup Statistical Findings

Outcome Domain	Main Finding	Statistical Interpretation
Tensile strength	Highest in chitosan–GO	$p < 0.05$
Water uptake	Lowest in chitosan–rGO; balanced in chitosan–GO	$p < 0.05$
Zone of inhibition	Highest in chitosan–GO across all organisms	$p < 0.05$
Direct-contact bacterial reduction	Highest in chitosan–GO at all time intervals	$p < 0.05$
Surviving bacterial count	Lowest in chitosan–GO	$p < 0.05$
Cell viability	Highest in pure chitosan; better preserved in chitosan–GO than rGO	$p < 0.05$
Hemolysis	Lowest in pure chitosan; lower in chitosan–GO than rGO	$p < 0.05$

Overall, the order of antimicrobial performance was chitosan–GO > chitosan–rGO > pure chitosan, while the order of biocompatibility was pure chitosan > chitosan–GO > chitosan–rGO. When antimicrobial, mechanical, and compatibility outcomes were interpreted together, chitosan–GO showed the most favorable translational profile.

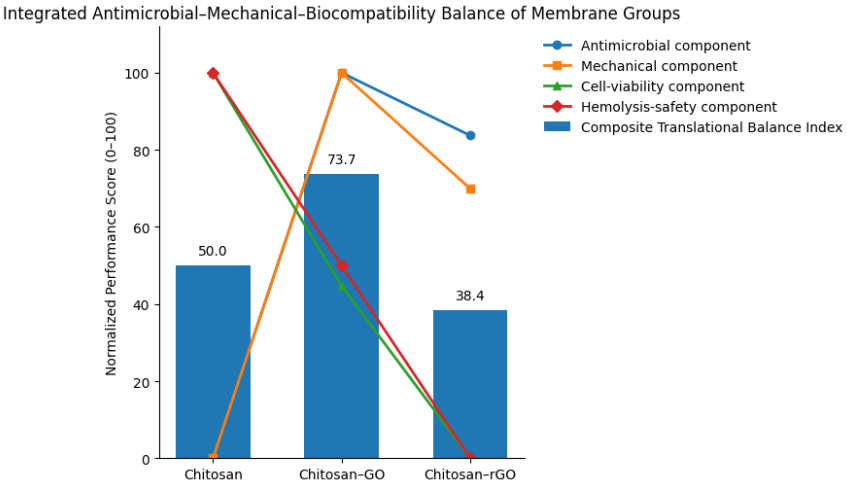

Figure 1 Integrated Antimicrobial–Mechanical–Biocompatibility Balance of Membrane Groups

The integrated performance profile showed that chitosan–GO achieved the highest composite translational balance index at 73.7, compared with 50.0 for pure chitosan and 38.4 for chitosan–rGO. This pattern reflects the superior combined performance of chitosan–GO, driven by the highest 24-hour bacterial reduction of 94.3%, greatest tensile strength of 32.7 MPa, acceptable cell viability of 88.7%, and controlled hemolysis of 2.6%. Although pure chitosan performed best in compatibility outcomes, its lower antimicrobial reduction and tensile strength reduced its overall translational suitability. Chitosan–rGO showed strong antibacterial activity but had a less favorable safety profile, with cell viability declining to 84.9% and hemolysis increasing to 3.4%.

DISCUSSION

The present study demonstrated that graphene reinforcement substantially improved the antimicrobial and mechanical performance of chitosan membranes, with the chitosan–graphene oxide membrane showing the most favorable overall profile. Compared with pure chitosan, both graphene-containing membranes produced larger zones of inhibition, greater time-dependent bacterial reduction, lower surviving bacterial counts, and higher tensile strength, confirming that graphene-based reinforcement improves both biological and structural membrane behavior. The superiority of chitosan–GO was most evident in direct-contact testing, where bacterial reduction reached 94.3 ± 2.8% after 24 hours compared with 88.5 ± 3.1% for chitosan–rGO and 58.7 ± 4.0% for pure chitosan. This finding supports the study hypothesis that graphene oxidation state influences antimicrobial performance, with GO providing a more effective balance of bacterial inhibition, polymer compatibility, and biological safety.

The moderate antimicrobial effect observed in the pure chitosan membrane was expected because chitosan is intrinsically antibacterial. Its positively charged amino groups interact with negatively charged bacterial cell envelopes, causing membrane permeability changes, leakage of intracellular components, and interference with normal microbial metabolism (17–21). However, the weaker inhibition zones and lower 24-hour bacterial reduction in the pure chitosan group indicate that chitosan alone may be insufficient where stronger infection-control performance and mechanical durability are required. This limitation is particularly relevant for wound-contact and biomedical surface applications, where materials must withstand moisture exposure, handling stress, and sustained bacterial challenge.

The stronger performance of the chitosan–GO membrane can be explained by the oxygen-containing functional groups present on graphene oxide. Hydroxyl, epoxy, and carboxyl groups improve hydrophilicity, dispersion, and interfacial bonding within the chitosan matrix, producing a more uniform membrane structure and more consistent bacterial contact (7,8,11,12). GO may also enhance bacterial killing through membrane stress, oxidative injury, wrapping or trapping effects, and disruption of cell-surface integrity (2,4,5,9,10). In the present study, chitosan–GO produced the highest tensile strength at 32.7 ± 2.1 MPa and the highest elongation at break at 24.6 ± 1.7%, indicating that its antimicrobial advantage was accompanied by improved mechanical integrity rather than structural compromise.

Chitosan–rGO also showed clear improvement over pure chitosan, but it remained slightly inferior to chitosan–GO in most antimicrobial, mechanical, and compatibility outcomes. Reduced graphene oxide contains fewer oxygenated functional groups and is generally less hydrophilic than GO, which may reduce dispersion uniformity and interfacial interaction with chitosan (2,3,6,11). This may explain why the rGO membrane showed lower water uptake but also slightly lower flexibility, reduced cell viability, and higher hemolysis compared with the GO membrane. The results suggest that excessive reduction of graphene oxide may improve hydrophobic stability but can reduce the biological and structural balance required for biomedical membrane design.

The organism-wise findings were clinically meaningful. Staphylococcus aureus was the most sensitive organism, while Pseudomonas aeruginosa showed the greatest resistance across membrane groups. This pattern is consistent with known bacterial structural differences, as Gram-negative organisms possess an additional outer membrane barrier, and P. aeruginosa is recognized for adaptive resistance mechanisms in hospital environments (2,5,17). Even so, both graphene-reinforced membranes produced substantial reductions in P. aeruginosa survival compared with pure chitosan, supporting their potential relevance against difficult hospital pathogens.

Biocompatibility findings showed that pure chitosan remained the most compatible material, with the highest cell viability and lowest hemolysis. However, the chitosan–GO membrane provided the better translational compromise because it retained acceptable cell viability at 88.7 ± 2.8% and hemolysis at 2.6 ± 0.4%, while also achieving superior antimicrobial and mechanical outcomes. Chitosan–rGO showed stronger antimicrobial performance than pure chitosan but had relatively lower cell viability and higher

hemolysis, suggesting that antimicrobial enhancement alone should not be considered sufficient for biomaterial selection. For clinical translation, the optimal membrane should balance bacterial control with host-tissue safety.

This study has several limitations. First, the work was conducted under in vitro experimental conditions, so the findings cannot directly predict clinical wound-healing performance or tissue response. Second, only selected bacterial species were tested, and broader evaluation against multidrug-resistant clinical isolates would strengthen external validity. Third, the study did not include advanced mechanistic assays for oxidative stress, membrane disruption, or biofilm inhibition. Fourth, although basic compatibility screening was included, long-term cytotoxicity, inflammatory response, and in vivo safety were not assessed. Future studies should include dose optimization, scanning electron microscopy, Fourier transform infrared spectroscopy, X-ray diffraction, thermal analysis, biofilm models, and animal wound models before clinical application is considered.

Overall, the findings indicate that graphene oxidation state is a critical determinant of chitosan composite membrane performance. The chitosan–GO membrane offered the most favorable combination of antimicrobial efficacy, mechanical reinforcement, and acceptable biocompatibility, making it the strongest candidate among the tested groups for further antimicrobial biomaterial development.

CONCLUSION

This comparative experimental study showed that graphene reinforcement improves the antimicrobial and mechanical performance of chitosan membranes, but the oxidation state of graphene plays an important role in determining overall biomaterial behavior. Pure chitosan demonstrated good biocompatibility but weaker antimicrobial and mechanical performance, while both chitosan–GO and chitosan–rGO membranes showed stronger bacterial inhibition and improved tensile strength. Among all groups, the chitosan–graphene oxide membrane produced the highest zones of inhibition, greatest 24-hour bacterial reduction, strongest tensile profile, and a more favorable compatibility balance than chitosan–rGO. These findings suggest that chitosan–GO is the most suitable membrane system under the present experimental conditions and may be a promising candidate for future wound-care and hospital infection-control biomaterial applications after further biofilm, cytotoxicity, and in vivo validation.

REFERENCES

1. Antimicrobial Resistance Collaborators. Global burden of bacterial antimicrobial resistance in 2019: a systematic analysis. Lancet. 2022;399(10325):629-655. doi:10.1016/S0140-6736(21)02724-0.

2. Liu S, Zeng TH, Hofmann M, Burcombe E, Wei J, Jiang R, et al. Antibacterial activity of graphite, graphite oxide, graphene oxide, and reduced graphene oxide: membrane and oxidative stress. ACS Nano. 2011;5(9):6971-6980. doi:10.1021/nn202451x.

3. Mokkapati VRSS, Pandit S, Kim J, Martensson A, Lovmar M, Westerlund F, et al. Bacterial response to graphene oxide and reduced graphene oxide integrated in agar plates. R Soc Open Sci. 2018;5:181083. doi:10.1098/rsos.181083.

4. Ravikumar V, Mijakovic I, Pandit S. Antimicrobial activity of graphene oxide contributes to alteration of key stress-related and membrane bound proteins. Int J Nanomedicine. 2022;17:6707-6721. doi:10.2147/IJN.S387590.

5. Metselaar HS, van der Kooi-Pol MM, Busscher HJ, Sharma PK, van Kooten TG, et al. Antibacterial activity of graphene oxide nanosheet against multidrug resistant hospital pathogens. R Soc Open Sci. 2020;7:200640. doi:10.1098/rsos.200640.

6. Mann R, Mitsidis D, Xie Z, McNeilly O, Ng YH, Amal R, et al. Antibacterial activity of reduced graphene oxide. J Nanomater. 2021;2021:9941577. doi:10.1155/2021/9941577.

7. Zuo PP, Feng HF, Xu ZZ, Zhang LF, Zhang YL, Xia W, et al. Fabrication of biocompatible and mechanically reinforced graphene oxide-chitosan nanocomposite films. Chem Cent J. 2013;7:39. doi:10.1186/1752-153X-7-39.

8. Han D, Yan L, Chen W, Li W. Preparation of chitosan/graphene oxide composite film with enhanced mechanical strength in the wet state. Carbohydr Polym. 2011;83(2):653-658. doi:10.1016/j.carbpol.2010.08.038.

9. Ruiz S, Tamayo JA, Delgado Ospina J, Navia Porras DP, Valencia Zapata ME, Mina Hernandez JH, et al. Antimicrobial films based on nanocomposites of chitosan/poly(vinyl alcohol)/graphene oxide for biomedical applications. Biomolecules. 2019;9(3):109. doi:10.3390/biom9030109.

10. Wrońska N, Anouar A, El Achaby M, Zawadzka K, Kędzierska M, Miłowska K, et al. Chitosan-functionalized graphene nanocomposite films: interfacial interplay and biological activity. Materials. 2020;13(4):998. doi:10.3390/ma13040998.

11. Feng W, Wang Z. Biomedical applications of chitosan-graphene oxide nanocomposites. iScience. 2022;25(2):103629. doi:10.1016/j.isci.2021.103629.

12. Valencia AM, Valencia CH, Zuluaga F, Grande-Tovar CD. Synthesis and fabrication of films including graphene oxide functionalized with chitosan for regenerative medicine applications. Heliyon. 2021;7(5):e07058. doi:10.1016/j.heliyon.2021.e07058.

13. Zambrano-Andazol I, Vázquez N, Chacón M, Sánchez-Avila RM, Persinal M, Blanco C, et al. Reduced graphene oxide membranes in ocular regenerative medicine. Mater Sci Eng C. 2020;114:111075. doi:10.1016/j.msec.2020.111075.

14. Jin L, Chen Q, Hu X, Chen H, Lu Y, Zhang Y, et al. Enhanced mechanical strength and antibacterial properties of chitosan/graphene oxide composite fibres. Cellulose. 2022;29:3889-3900. doi:10.1007/s10570-022-04523-8.

15. Gong Y, Yu Y, Kang H, Chen X, Liu H, Zhang Y, et al. Synthesis and characterization of graphene oxide/chitosan composite aerogels with high mechanical performance. Polymers. 2019;11(5):777. doi:10.3390/polym11050777.

16. Yang Y, Dong Z, Li M, Liu L, Luo H, Wang P, et al. Graphene oxide/copper nanoderivatives-modified chitosan/hyaluronic acid dressings for facilitating wound healing in infected full-thickness skin defects. Int J Nanomedicine. 2020;15:8231-8247. doi:10.2147/IJN.S278631.

17. Confederat LG, Tuchiluş CG, Drăgan M, Sha'at M, Dragostin OM. Preparation and antimicrobial activity of chitosan and its derivatives: a concise review. Molecules. 2021;26(12):3694. doi:10.3390/molecules26123694.

18. Chitosan and its derivatives: preparation and antibacterial properties. Materials. 2023;16(18):6076. doi:10.3390/ma16186076.

19. Rajoka MSR, Zhao L, Mehwish HM, Wu Y, Mahmood S. Chitosan and its derivatives: synthesis, biotechnological applications, and future challenges. Appl Microbiol Biotechnol. 2019;103:1557-1571. doi:10.1007/s00253-018-9550-z.

20. Bakshi PS, Selvakumar D, Kadirvelu K, Kumar NS. Chitosan as an environment friendly biomaterial: a review on recent modifications and applications. Int J Biol Macromol. 2020;150:1072-1083. doi:10.1016/j.ijbiomac.2019.10.113.

21. Khubiev OM, Egorov AR, Kirichuk AA, Khrustalev VN, Tskhovrebov AG, Kritchenkov AS. Chitosan-based antibacterial films for biomedical and food applications. Int J Mol Sci. 2023;24(13):10738. doi:10.3390/ijms241310738.

22. Ng IMJ, Shamsi S. Graphene oxide: a promising nanomaterial against infectious diseases caused by multidrug-resistant bacteria. Int J Mol Sci. 2022;23(16):9096. doi:10.3390/ijms23169096.

23. Bilal H, Khan MN, Rehman T, Hameed MF, Yang X. Antibiotic resistance in Pakistan: a systematic review of past decade. BMC Infect Dis. 2021;21:244. doi:10.1186/s12879-021-05906-1.

24. Salahuddin N, Khalid M, Baig-Ansari N, Iftikhar S, et al. Five-year audit of infectious diseases at a tertiary care hospital in Karachi, Pakistan. Cureus. 2018;10(11):e3551. doi:10.7759/cureus.3551.

25. Zehra A, Ansari T, Shah SSAM, Syed B, Rizvi M, Anjum F, et al. Antibiotic stewardship benchmarking: using the WHO point prevalence survey of antimicrobial prescribing in a tertiary care public hospital, Karachi. PLoS One. 2026. doi:10.1371/journal.pone.0342985.